



Hydrogen as a Nuclear Thermal Rocket Propellant

Rezende^a P.A., Costa^a A.L., Marques^a G.O., Pereira^a C., Barros^b J.E.M.

^a Universidade Federal de Minas Gerais / Departamento de Engenharia Nuclear

^b Universidade Federal de Minas Gerais / Departamento de Engenharia Mecânica

Av. Antônio Carlos, 31270-901, Belo Horizonte, Minas Gerais, Brazil

antonella@nuclear.ufmg.br

ABSTRACT

Nuclear Thermal Propulsion (NTP) has been extensively ground-tested and is a successfully developed technology, though it hasn't been officially used in a propulsion system of a space mission. In spite of that, it is the technology most likely to make long distance journeys in space possible. It is considerably more efficient than the traditional chemical rocket engines, regarding propellant consumption for each unit of thrust generated. The reason for that is the greater number of choices regarding the propellant composition. In this work, Hydrogen has been chosen as propellant due to its low molecular mass compared to other possible substances. The aim is to explain how the propellant molecular mass impacts a rocket performance, and to show, by the deduction of an expression for exhaust velocity and an example of Computational Fluid Dynamics (CFD) simulations that, indeed, hydrogen seems to be the best choice available among possible nuclear thermal rocket propellants.

Keywords: Nuclear Thermal Propulsion, Computational Fluid Dynamics, Hydrogen.



1. INTRODUCTION

Nuclear Thermal Propulsion (NTP) is a promising technology that is expected to be one of the best propulsion alternatives for the near future regarding long range space missions. The main reason for that is the high performance on propellant consumption. This characteristic allows the spacecraft to reach higher speeds which can dramatically reduce the mission duration, when compared with combustion propelled rockets. Hence, the propellant choice clearly plays an important role in NTP efficiency. Hydrogen is a strong candidate as a propellant due, mainly, to its low molecular mass [2]. The purpose of this paper is to demonstrate why that is the case and how that conclusion is reached.

The work was performed through the deduction of Equation 1 that relates molecular mass to efficiency while explaining the assumptions made to do so, and the CFD simulation of the Kiwi A reactor, the first reactor built in the Rover program [1, 3] as an example. The results demonstrate quantitatively the hydrogen performance compared to other fluids, like water vapor and air.

2. MATERIALS AND METHODS

2.1. The Exhaust Velocity Equation

In this Section, Equation 1, which makes explicit the relation between exhaust velocity and the ratio between nozzle inlet temperature and propellant molecular mass, is deduced from isentropic and control volume thermodynamics and from ideal gas relations [4, 5, 6].

$$V_e = \sqrt{\frac{T_i}{\mathcal{M}}} \cdot \sqrt{2 \cdot \frac{k \cdot \mathcal{R}}{k-1} \cdot \left(1 - \left(\frac{p_e}{p_i}\right)^{\frac{k-1}{k}}\right) + V_i^2} \quad (1)$$

In Equation 1, V_e is the exhaust velocity (m/s), T_i is the inlet temperature (K), \mathcal{M} is the propellant molecular mass (g/mol), k is the propellant specific heat ratio, \mathcal{R} is the universal gas constant (J/K.mol), p_e is the exit pressure (Pa), p_i is the inlet pressure (Pa) and V_i is the inlet velocity (m/s).

To deduce Equation 1, one starts with Equation 2 which provides that:

$$\vec{T}_{\text{momentum}} = -\dot{m} \cdot \vec{V}_e \Rightarrow T_{\text{momentum}} = \dot{m} \cdot V_e \quad (2)$$

Where $\vec{T}_{\text{momentum}}$ is the force exerted on the rocket by the propellant exhaust. This force is complemented by another exerted by the pressure difference between the nozzle exhaust and the exterior pressure. Therefore:

$$T = \dot{m} \cdot V_e + (p_e - p_{\text{out}}) \cdot A_e \quad (3)$$

where, in Equation 3, p_{out} is the pressure outside, p_e is the pressure at the nozzle exhaust, and A_e is the nozzle exhaust area.

Analyzing the nozzle as a control volume, from the first law of thermodynamics, the energy rate balance can be represented by Equation 4:

$$\frac{dE_{\text{cv}}}{dt} = \dot{Q} - \dot{W} + \dot{m} \cdot \left(u_{\text{in}} + \frac{V_{\text{in}}^2}{2} \right) - \dot{m} \cdot \left(u_e + \frac{V_e^2}{2} \right) \quad (4)$$

where \dot{Q} is the heat transfer rate, \dot{W} is the work rate, u is the internal energy at the subscript location, V and is the velocity at the subscript location. Subscript "in" refers to inlet, and "e" refers to exhaust.

In this case, the nozzle is considered adiabatic, that is, \dot{Q} is zero. Also, the system operates at steady state, meaning there is no energy change rate.

Due to control volume nature, work is always done by or on the system when mass is inserted or expelled through its boundaries. Therefore, work is split into two categories, work done through mass flow, and every other kind of work that remains. Note that in this case there is no work other than that due to mass flow. Work rate can then be rewritten as in Equation 5:

$$\dot{W} = \dot{W}_{\text{else}} + \dot{m} \cdot (p_e \cdot v_e) - \dot{m} \cdot (p_{\text{in}} \cdot v_{\text{in}}) \quad (5)$$

where v is the specific volume at subscript location.

Enthalpy is defined as in Equation 6:

$$H = U + P \cdot V \stackrel{\dot{m}}{\Rightarrow} h = u + p \cdot v \quad (6)$$

Through Equation 5 and the definition of enthalpy in Equation 6, Equation 4 simplifies to:

$$h_{\text{in}} - h_e = \frac{1}{2} \cdot (V_e^2 - V_{\text{in}}^2) \quad (7)$$

Entropy rate balance for the control volume is given by Equation 8:

$$\frac{dS_{\text{cv}}}{dt} = \sum_i \frac{\dot{Q}_i}{T_i} + \dot{m} \cdot s_{\text{in}} - \dot{m} \cdot s_e + \dot{\sigma}_{\text{cv}} \quad (8)$$

where S_{cv} is the total entropy inside the control volume, \dot{Q}_i is the heat transferred through control volume boundary "i", T_i is the temperature of control volume boundary "i", s is the specific entropy at subscript location, and $\dot{\sigma}_{\text{cv}}$ is the entropy generation inside the control volume.

The nozzle operates in steady state and is, as previously mentioned, considered adiabatic. Moreover, its internal processes are considered reversible. Therefore, Equation 8 simplifies to:

$$s_{\text{in}} = s_e \quad (9)$$

Hence, the nozzle is isentropic.

From an energy balance over a simple compressible system with internal reversible processes, the Tds equations are easily derived resulting in:

$$T \cdot ds = du + p \cdot dv \quad (10)$$

$$T \cdot ds = dh - v \cdot dp \quad (11)$$

Considering that the working fluid is an ideal gas and that specific heats are constant:

$$du = c_v \cdot dT, dh = c_p \cdot dT, p \cdot v = R \cdot T \quad (12)$$

Equation 12 can be implemented in Equation 11, and then integrated to get to the Equation 13:

$$s_e - s_{in} = c_p \cdot \ln \left(\frac{T_e}{T_{in}} \right) - R \cdot \ln \left(\frac{p_e}{p_{in}} \right) \quad (13)$$

Considering Equation 9 and since for an ideal gas:

$$c_p = \frac{k \cdot R}{k-1} \quad (14)$$

then, Equation 13 leads to Equation 15:

$$\frac{T_e}{T_{in}} = \left(\frac{p_e}{p_{in}} \right)^{\frac{k-1}{k}} \quad (15)$$

Solving Equation 7 for V_e :

$$V_e = \sqrt{2 \cdot (h_{in} - h_e) + V_{in}^2} \quad (16)$$

Implementing ideal gas enthalpy relation in Equation 12 into Equation 16:

$$V_e = \sqrt{2 \cdot c_p \cdot (T_{in} - T_e) + V_{in}^2} \quad (17)$$

Solving Equation 15 for T_e and implementing it together with Equation 14 into Equation 17:

$$V_e = \sqrt{2 \cdot \frac{k \cdot R}{k-1} \cdot \left(T_{in} - T_{in} \cdot \left(\frac{p_e}{p_{in}} \right)^{\frac{k-1}{k}} \right) + V_{in}^2} \quad (18)$$

Factorizing T_{in} out:

$$V_e = \sqrt{2 \cdot \frac{k \cdot R}{k-1} \cdot T_{in} \cdot \left(1 - \left(\frac{p_e}{p_{in}}\right)^{\frac{k-1}{k}}\right) + V_{in}^2} \quad (19)$$

Finally, R can be replaced by $\frac{\mathcal{R}}{\mathcal{M}}$, where \mathcal{R} is the universal gas constant and \mathcal{M} is the propellant molecular mass, so that Equation 19 can be manipulated into:

$$V_e = \sqrt{\frac{T_{in}}{\mathcal{M}}} \cdot \sqrt{2 \cdot \frac{k \cdot \mathcal{R}}{k-1} \cdot \left(1 - \left(\frac{p_e}{p_{in}}\right)^{\frac{k-1}{k}}\right) + V_{in}^2} \quad (20)$$

which is exactly Equation 1.

2.2. Problem Setup and Feeding Equation 1

To feed Equation 1, data on the Kiwi A reactor tests was collected from [1]. The reactor dimensions were used to draw the 3D model, illustrated in Figure 1, used in the CFD simulation. Moreover, reactor power and mass flow data were used to estimate the test boundary conditions. In that sense, it was assumed that the reactor operated in steady state conditions, and, therefore, the reactor internal walls were supposed to heat the propellant with a constant heat flux throughout the reactor. The Kiwi A reactor consisted of a sequence of 3 “whims” (the structure illustrated in Figure 1 loaded with 4 micrometers sized UO_2 particles (their density was about 10.3 g/cm^3), followed by one unloaded whim [1, 3]. The level of enrichment is estimated at 93% [1]. For the sake of simplicity and due to symmetry, only 1/24 of a whim was simulated. It is enough to make the intended point. It is important to note that the reactor was simulated in test conditions, which are very different from operation conditions on potential missions. The same problem was simulated using 3 different propellants: air, water vapor and hydrogen. It was considered that the energy absorbed by the fluid was all off the energy generated by the reactor (the generated power value was collected from reactor

test reports [1]) evenly distributed through the fuel plates surfaces ($1,477,050 \text{ W/m}^2$). The other boundary conditions were: 0.133 kg/s inlet mass flow [1]; 0° C average inlet temperature; and 1 atm outlet absolute pressure. Moreover, the mesh was composed by tetrahedrons with sizing set to 0.003 m into Ansys Mesh. Inflation was added to the mesh inside the flow channels between the plates. It was composed by eight layers with a growth factor of 1.2 to smoothly transition to the general mesh element size. The convergence criteria were set to $E-03$ for all of the residuals since it was enough to assure the outlet average temperature and mass flow rates had reached stable values (moreover, the mass flow balance across the boundaries was close to 0). These criteria were taken in the absence of any reference regarding convergence criteria for this very specific problem. The turbulence model used was the realizable k-epsilon model which was the default model set in Fluent. The model coefficients were the default as well. This approach was taken due to the, once again, absence of data regarding appropriate coefficients for the turbulence model in this example, and since there seem to be no clear indication against the realizable k-epsilon model application in this specific problem the turbulence model was not changed nor the standard coefficients which intent is to cover a wide range of problems.

Since the temperature results in this example were close for all propellants as expected, clearly showing the intended point of this paper, and due to the lack of data to compare the results to, no actions were taken to further improve the results accuracy either by reducing error originated by spots of poor mesh quality, or by changing model parameters such as the turbulence model or its coefficients. These actions would overcomplicate an example which only objective is to show the trend in the results which point to hydrogen being more efficient. Furthermore, to adequately determine appropriate convergence criteria and turbulence model coefficients would require extensive testing which, once again, is not the intent of this paper.

The most important result from the simulation is the average temperature in the reactor outlet, which would be the nozzle inlet if one was attached, since molecular mass is already known. These 2 variables define $\sqrt{\frac{T_{in}}{M}}$ in Equation 1. This factor is responsible for most of the impact on the exhaust velocity due to change in the propellant. Hence, this factor is calculated for each propellant using the

results from the simulations and then compared with one another. Moreover, the simulations allow for an analysis of the propellant mechanical behavior inside the reactor, and for detection of heat concentration points.

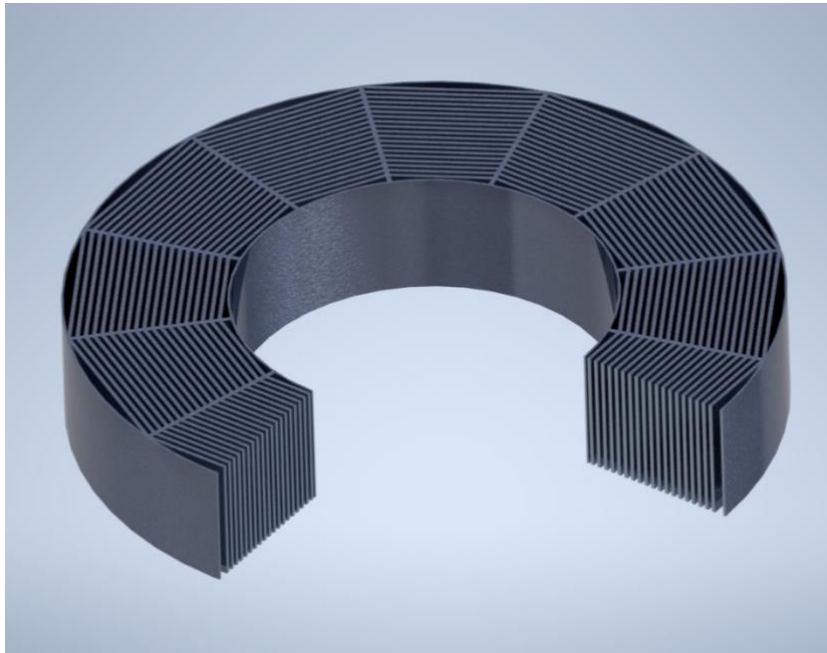


Figure 1: A sectional view of the 3D drawing of the KIWI A 84 cm diameter whim.

3. RESULTS AND DISCUSSION

As expected, the results show that hydrogen has a higher ratio between average reactor outlet temperature and molecular mass. The ratio for each propellant is shown in Table 1.

Once again, the intent of the average temperature values calculated is not to match the reported temperature values, since this reactor test was terminated due to fuel overheating [1]. Moreover, the boundary conditions, like the propellant inlet temperature, are mostly unknown and, therefore, these values should be treated as rough estimates. Despite all of that, since the propellants were simulated under the same conditions, it seems enough to show that exhaust velocity would be more than 3 times higher for hydrogen when compared to water vapor and air. This means that a nuclear rocket propelled

by hydrogen needs less than 1/3 of the propellant mass that a water vapor or air-cooled nuclear rocket would need to generate the same thrust.

Table 1: Propellant properties and average outlet temperature results.

Propellant	Molecular Mass [7] (g/mol)	Simulated Reactor	
		Outlet Average Temperature (K)	$\sqrt{\frac{T_i}{M}}$ (K.mol/g) ^{1/2}
Air	28.97	2605	9.48
Water Vapor	18.02	2328	11.37
Hydrogen	2.016	2363	34.27

4. CONCLUSION

The results confirmed the expected relation between hydrogen and other propellants: it is a lot more efficient. The results are specifically interesting because they match very closely the comparison made by Corliss and Scwenk [2], between a combustion rocket that burns hydrogen with oxygen, expelling water through the nozzle, and a nuclear rocket using hydrogen. It was estimated that hydrogen would be 3 times more efficient than water. Moreover, the results show that indeed, the KIWI A reactor would probably suffer from overheating, which was the reason its real tests were terminated.

ACKNOWLEDGMENT

The authors are grateful to the *Coordenação de Aperfeiçoamento de Pessoal de Nível Superior* (CAPES), to *Fundação de Amparo à Pesquisa do Estado de Minas Gerais* (FAPEMIG), to *Conselho Nacional de Desenvolvimento Científico e Tecnológico* (CNPq) and to *Comissão Nacional de*

Energia Nuclear (CNEN) for the support to the several research projects of the Nuclear Engineering Department of UFMG.

REFERENCES

- [1] FINSETH, J.L. **Overview of Rover Engine Tests – Final Report**, Huntsville & USA, 1991.
- [2] CORLISS, W. R.; SCHWENK, F.C. **Nuclear Propulsion for Space**, 1st ed. Washington & United States, Library of Congress, 1971.
- [3] KOENIG, D. R. **Experience Gained from the Space Nuclear Rocket Program (Rover)**, Los Alamos Scientific Laboratory, Los Alamos & United States, 1986.
- [4] TURNER, M. J. L. **Rocket and Spacecraft Propulsion**, 2nd ed. Chichester & United Kingdom, Springer – PRAXIS, 2006.
- [5] MORAN, M. J.; SHAPIRO, H. N.; BOETTNER, D. D.; BAILEY, M. B. **Engineering Thermodynamics**, 9th ed. Hoboken & United States, John Wiley & Sons, 2018.
- [6] SUTTON, G. P.; BIBLARZ, O. **Rocket Propulsion Elements**, 9th ed. Hoboken & United States, John Wiley & Sons, 2017.
- [7] Engineering Toolbox. **Molecular Weight of Substances**, 2009. Available at: <https://www.engineeringtoolbox.com/molecular-weight-gas-vapor-d_1156.html>. Last accessed: 12 Jan. 2022.